APPLICATION OF FINITE ELEMENT METHODS FOR THE ANALYSIS OF THERMAL CREEP, IRRADIATION INDUCED CREEP, AND SWELLING FOR LMFBR DESIGN

J.A. SWANSON,
Swanson Analysis Systems, Inc., Elizabeth, Pennsylvania, U.S.A.

J.F. PATTERSON,
Westinghouse Electric Corporation,
Atomic Power Divisions, Madison, Pennsylvania, U.S.A.

ABSTRACT

The finite element method provides a valuable tool for the analysis of the many interacting effects which occur in the design analysis of the Liquid Metal Fast Breeder Reactor (LMFBR). The material effects which are discussed in this paper include the usual elastic and thermal effects, thermal and irradiation induced creep, swelling due to the fast neutron fluence, and plasticity. In addition two different geometric effects are sometimes needed - large deflections and interface interactions.

The first section of the paper discusses the methods which are used to treat these effects and their interactions. The second section of the paper illustrates the application of these methods to actual LMFBR design analyses. Included in this second section are examples of analyses of fuel rods and fuel assembly ducts.

1. INTRODUCTION

The finite element method has demonstrated its usefulness in the elastic analysis of structures, both statically and dynamically. This paper presents examples of the application of the finite element methods to a class of design analysis for which non-linear effects are of prime importance. These non-linear effects are both material non-linearities and geometric non-linearities. The material non-linearities include plasticity, thermal creep, irradiation induced creep, and swelling. The geometric non-linearities include the geometric changes caused by large deformations and the stiffness changes induced by interfaces which may or may not be in contact during a particular portion of the operating cycle.

This paper presents the techniques which are used to analyze the combined effects of these interactions and then presents results obtained when these techniques are applied to design analyses in the LMFBR fuel rods and ducts.

2. METHODS

The first part of this section discusses the various types of non-linearities which are utilized in the LMFBR core analyses and the second part shows how these effects are combined. The ANSYS computer program, developed by Swanson [1], is used as an example.

2.1 Individual Effects

2.1.1 Irradiation Induced Swelling

The phenomenon of irradiation induced swelling was first observed in Type 316 stainless steel clad fuel rods in DFR, as reported by Cawthorne and Fulton [2]. Since then the effect has been observed in other stainless steels, nickel base alloys, aluminum and vanadium. Although the mechanisms that lead to swelling are not well understood, there is general agreement that a supersaturation of point defects is produced by irradiation, leading to enhanced point defect migration and agglomeration. Helium produced by (n, α) reactions may help to stabilize small vacancy clusters which would otherwise redissolve in the lattice. These vacancy clusters would then grow upon further diffusion of vacancies, leading to voids containing only a small partial pressure of gas.

Electron microscopy observations reported by Bloom [3], indicates these voids are typically 100-1000 Å in diameter and cause a decrease in the apparent density of the material. Void formation in irradiated stainless steels has only been observed in the range 370 - 750°C after fast fluences on the order of 10^{22} n/cm^2.

Boltax et al. [4,5] has proposed models for irradiation induced swelling. The following model proposed by A. Boltax et al.[5] for the stress-free swelling of the stainless steel is

$$\frac{\Delta L}{L} = C_1 (\phi t)^{C_2} [C_3 - C_4 T + C_5 T^2 - C_6 T^3] \qquad (1)$$

where

$\Delta L/L$ is the swelling strain length

ϕt is fast fluence (> 0.1 MeV), n/cm^2

T is the temperature, °K

$C_1 - C_6$ are constants of the material having the following estimated values for Type 316 cold worked stainless steel:

$C_1 = 3 \times 10^{-37}$

$C_2 = 1.5$

$C_3 = 4.028$

$C_4 = 3.712 \times 10^{-2}$

$C_5 = 1.0145 \times 10^{-4}$

$C_6 = 7.879 \times 10^{-8}$

A swelling of this form is quite analogous to a thermal strain due to a temperature increase, and is treated in the same way. The fluence is input to the computer program as a "temperature" and the swelling strain (ε_{sw}) is calculated from Equation (1).

2.1.2 Plasticity

The treatment of plasticity in the ANSYS program is based on the incremental technique outlined by Mendelson.[6] This procedure can be summarized as follows:

a. Calculate the elastic stress distribution including the effects of previous non-linear strains and the present values of the thermal and swelling strains.

b. For each element, evaluate the stresses and compare the equivalent stress with the stress-strain relationship for the material (expressed in tabular form as a function of temperature and strain). If the stress is within the yield surface, the stress state is elastic and no additional plastic strain occurs. If the stress state is outside the yield surface a plastic strain increment is calculated which will make the element stress state consistent with the stress-strain relationship. A new elastic stress is then calculated from the old elastic strain less the plastic strain increment. Steps a and b are then repeated for the next load step.

This procedure is illustrated in Figure 1, where A-B is the plastic strain due to previous load steps, B-D is the calculated elastic strain for this load step, producing a stress which lies above the stress-strain curve. This calculated elastic strain is separated into a new elastic component C-D which is consistent with the stress-strain relationship and a plastic strain increment B-C which is added to the previous plastic strain.

The convergence of this process is rapid for deformation-limited stress states, such as for thermal stresses, but is slow for load-limited stress states, such as for primary stresses, especially if the stress-strain curve is relatively flat. An option may be selected which greatly reduces the number of iterations required for convergence to a plastic solution. In this improved technique the load is incremented in a uniform manner and the displacements and strains at the next load point are extrapolated from the conditions at the present load point. The plastic strain for the next step is then estimated based on this extrapolation and this estimate is used in the calculation of the displacement and strain conditions at the next load point. These extrapolated strains are a much better estimate of the actual plastic strains at the next load point than the plastic strains at the present load point would be, so the deviation from the stress-strain curve at the next point is much reduced. Reduction of a factor of 5 in the number of iterations required for a given level of convergence are easily obtained with this technique.

An advantage of the incremental technique of plasticity is the ease with which unloading is accomplished. Since each load step is an elastic solution of the elasticity problem, unloading is the direct output of the elastic solution with no corrections required.

The behavior of the material under reversed loading has been discussed by many authors. Rather than a select one approach and limit the analyst to that choice the ANSYS program offers three options for the material behavior. These options are illustrated in Figure 2. Curve A is an approximation to kinematic hardening, where the total stress range is twice the original yield stress. Curve B shows no effect of the tensile yielding on the compressive behavior - the virgin stress-strain curve is used for the reversed loading. Curve C is isotropic hardening - yielding does not occur in the reversed loading direction until the stress reaches the highest value reached in any previous cycle.

2.1.3 Creep

Two types of creep are used in the LMFBR analysis - thermal creep, in which the creep rate depends only on the stress and the temperature level, and irradiation induced creep, where the creep rate also depends on the fluence.

a. Secondary Thermal Creep

One of the major long-term mechanical properties, and a life limiting factor for many LMFBR structures, is the secondary thermal creep rate. Available secondary creep rate data on both solution-treated and 20% cold worked material were analyzed graphically and various mechanical models were employed to describe the data. A slight modification of the sinh function, discussed by Garafalo [7], gave the best statistical fit of the data. The equation has the following form:

$$\dot{\varepsilon}_{cr} = C_1 \exp\,(C_2/T) \left\{ \sinh \left(\frac{C_3\, \bar{\sigma}}{T} \right) \right\}^{C_4} \qquad (2)$$

where

T is the temperature, °K

$\bar{\sigma}$ is the equivalent stress, psi

$\dot{\varepsilon}_{cr}$ is the equivalent creep strain rate, hr^{-1}

$C_1 - C_4$ are material constants having the following values for Type 316 cold worked stainless steel:

$C_1 = 6.55 \times 10^{14}$

$C_2 = 4.487 \times 10^{4}$

$C_3 = 0.3$

$C_4 = 1.0$

b. Irradiation Induced Creep

Enhanced strain under neutron irradiation is a well-recognized phenomenon, and has been observed directly and indirectly in many materials. However, quantitative data, and data applicable to LMFBR's, are limited. Available data includes that of Mosedale et al.[8] for cold worked Type 316 stainless steel helical springs irradiated at 250°C and data from fuel rods irradiated in the EBR-II and DFR reactors.

Hesketh[9] has proposed that the transient creep strain saturates after dislocation climb by vacancy and interstitial absorption has saturated. The analysis of the available stainless steel data indicated that in-reactor creep can be considered as the sum of a transient strain component which saturates at low fluence and a steady state strain.[4] The data are fit to an equation of the form

$$\varepsilon_i = \frac{C_1}{T}\sigma[1-\exp(-\phi t/C_2 T)] + \frac{C_3}{T}\sigma\phi t \qquad (3)$$

where

ε_i is irradiated-induced creep, (in/in)

σ is the stress, psi

ϕt is the fast fluence (> 0.1 MeV), n/cm^2

T is temperature, °K

$C_1 - C_3$ are material constants having the following values for type 316 cold worked stainless steel:

$C_1 = 1.046 \times 10^{-5}$

$C_2 = 4.2 \times 10^{17}$

$C_3 = 2.25 \times 10^{-27}$

The creep rates are calculated on the elastic stresses remaining after the plastic strain components have been subtracted. Having determined the creep rate(s) based on the present stresses in the system of finite elements, the analyst may select either of two options, depending upon the physical conditions being considered, for the behavior of the elements as a result of the creep which occurs during the next time interval. He may assume that the stresses are independent of the creep, and thus that the calculated creep rate is maintained over the complete time interval. The total creep strain increments are then the creep rates times the length of the interval. This assumption is illustrated by the dashed line in Figure 3. Alternatively, the user may assume that the stresses decay as the creep occurs, giving a decay type of curve as illustrated by the solid curve in Figure 3. This procedure gives rapid convergence for strain induced stresses, such as thermal stresses, but can seriously underestimate the creep strains due to primary stresses. As can be seen from the figure the results from the two assumptions should be the same for small time intervals.

Large time increments with the constant stress assumption can lead to a divergent oscillation in the creep solution. This can occur when the creep strain increment is more than twice the elastic strain, producing a reversed strain which is bigger in magnitude than the original stress, and thus starting the divergent oscillation. However, the use of this linear option tends to assure a reasonable solution, because a time step size small enough to avoid this instability usually leads to a good creep solution.

2.1.4 Interfaces

In many analyses it is desirable to be able to treat gaps which may open and close during the analysis internally in the computer program, rather than having to make manual model adjustments to compensate for the changing configurations. This may be done in the ANSYS program by special elements which are called "interface elements". These elements have the force-deflection characteristics shown in Figure 4. The "stiffness" of these interface elements is made large relative to the stiffness of the rest of the structure. These interfaces can support no normal tensile force, and the shear force can be no more than the coefficient of friction times the interface contact force.

2.1.5 Large Deflections

Some analyses of LMFBR components have produced calculated displacements of large enough magnitude that the change in geometry has a significant effect on the loading. For these analyses a large deflection option in the program is used. This option updates the geometry at the end of each load step so that the next load step is applied to the revised geometry. Comparisons of the results with and without the geometry modification confirm that the effects of these geometry changes on the total deformation of the structure can be significant.

2.2 Combined Effects

The ANSYS computer program is a finite element program which includes all the effects discussed in the first part of this section and to do so in a manner such that a complete analysis can be done in a single computer run with no analyst intervention.

An overall flow chart for the most general type of static non-linear analysis is shown in Figure 5. The initial geometry definition includes the elements defining the structure (solids, beams, spars, shells, etc.), and the interface elements defining gaps between portions of the structure which are expected to interact. The material properties include the elastic constants (as a function of temperature), the temperature dependent stress-strain relationship, and the coefficients for the creep and swelling equations.

In the following two loops the outer loop defines the structure boundary conditions at various time points during the life of the structure. These may be specified displacements, forces, pressures and/or temperatures. The inner loop is the calculation

loop, and there may be several calculations for each set of boundary conditions, with linear interpolation used between boundary condition times.

Within this calculation loop the element and total stiffness (K) matrices are formed, with the interface stiffness depending on the status of the interface elements at the previous calculation point (open or closed, static or sliding). The element load vectors including the new thermal and swelling strains and the previous values of the creep and plastic strains are then formed, and the nodal displacement solution at this time point is calculated. From the nodal displacements the total strains in each element are determined and the element elastic strain is obtained. This elastic strain is compared with the stress-strain relationship at the appropriate temperature and a plastic strain increment is determined for those elements in which additional yielding occurs. The stress distribution is then found based on the remaining elastic stress components. The calculated interface forces and displacements are then checked and appropriate keys representing the interface state are set to be used for the next calculation cycle. The elastic stress distribution is then allowed to creep for the time increment between the previous calculation point and this point, and the creep strain increments are determined. These creep strain increments are subtracted from the elastic strains and the strain distributions are tabulated. Finally, the geometry is modified by the displacement increment which occurred in this time increment and then the entire calculation cycle repeats.

For many problems a simpler analysis procedure can be applied. These problems are those for which there are no interface elements, the deflections are small, and the displacement boundary conditions are all zero. For such problems the structure stiffness matrix can be determined once, and only the load vector need be recalculated at each calculation cycle. The flow chart for this shorter procedure is shown in Figure 6. A significant reduction in computer time can be realized with this simplified procedure.

3. APPLICATION OF TECHNIQUES

The environmental conditions present in an LMFBR present the designer with extremely difficult problems, which, in many cases, are unique to this type of a reactor. Development of a variable breeder industry will depend upon demonstrated component reliability which can be achieved, only if adequate analytical tools and material property data are available to the designer. Finite element methods are particularly adaptable for the analysis of complex, interrelated physical phenomena described in Section 2 and which must be considered in the design of an LMFBR.

Swelling complicates a reactor design because room must be provided in core region for significant dimensional changes. In addition, swelling can cause gross distortion of fuel assemblies thereby complicating the refueling process. On the other hand, swelling of fuel rod cladding reduces the probability of high loads due to fuel swelling, and perhaps even extends the burnup capability of a fuel rod.

Thermal and irradiation induced creep may be beneficial in some cases by permitting stress relaxation of components and thereby limiting distortions due to swelling. In other cases, one which is considered below, creep may cause structural distortions which are of considerable concern to the designer. Current data indicates that irradiation induced creep decreases with increasing temperature, the trend being opposite that displayed by thermal creep. This point is illustrated in Figure 7. Using models of the form presented in Section 2 above, irradiation induced creep and total creep was calculated as a function of stress level temperature for a total fast fluence (> 0.1 MeV) level of $2.0 \times 10^{23} n/cm^2$ for a period of 2.1 years.

Two illustrative examples of the application of finite element techniques in the design of an LMFBR are described below.

3.1 Fuel Rod Design

A hypothetical LMFBR fuel rod was analyzed to determine the effects of phenomena listed above. The major loading on the fuel rod cladding, in this case, was the gradual pressure buildup of fission product gases to a maximum of 800 psig at the end of two years. A peak cladding temperature of 1225°F was assumed. The ductility limited hoop strain, which includes primary and secondary thermal creep plus the effects of steady state thermal gradients, is shown in Figure 8. The strain is shown as a function of core height, with the hot end of the rod at the right of the figure. The solid line assumes worst case material properties and corrosion rates at an estimated two standard deviations about the mean for available data. The dashed line assumes mean material properties and corrosion rates.

The large differences between mean value results and results assuming 2σ limits (two standard deviations on the limits) illustrates the fact that, in many LMFBR design problems, material uncertainties are far more significant than uncertainties in analysis techniques.

Figure 9 includes all hoop strain including the effects of irradiation induced creep and swelling. It is useful for the designer to separate the latter two effects because it is generally accepted that they are not ductility limited effects and do not, in themselves, impose design limits as far as rupture strain.[4]

3.2 Fuel Assembly Duct Design

LMFBR fuel assemblies typically incorporate a closed hexagonal shaped duct which surrounds a bundle of fuel rods. These ducts may be subjected to significant pressure differentials causing primarily bending stresses.

In a hypothetical case, the ANSYS code was used to calculate duct deformation with irradiation to a fast fluence of $2.0 \times 10^{23} n/cm^2$ at a temperature of 900°F and a pressure differential of 80 psi. The effect of irradiation induced swelling on duct deformation is shown in Figure 10. Figure 11 shows the combined effect of swelling and creep based

upon models given in Section 2.

Note the significant degree of duct dilation of the center span of the flat in Figure 11. This is primarily due to high bending stresses in the duct. Again the uncertainties in the model are far more significant than uncertainties in the calculational procedures. For example, equation (3) above is based upon in-pile irradiation samples subjected to shear stresses in the case of Mosedale's spring data [7] and in-pile data for fuel rods subjected to tension stresses. Currently there is no pertinent in-pile data for samples subjected to bending stresses. Furthermore, available material property data in general, extends to fluences of about one-third current goals for current LMFBR designs.

4. CONCLUSIONS

Finite element techniques provide the means for analyzing the combined effects of material and geometric non-linearities which are encountered in LMFBR design. Computer programs such as the ANSYS program provide the designer and analyst with the analytical tools required to study the effects of these non-linearities in the reactor design and operation. However, the results from any analysis can be no better than the material properties and behavior postulated for the materials, and much effort will be required in the study of the materials used in the LMFBR before the material behavior can be specified with the accuracy desired for final detailed design analyses.

REFERENCES

[1] Swanson, J. A., ANSYS-Engineering Analysis System, Swanson Analysis Systems, Inc., 1971.

[2] Cawthorne, C. and Fulton, E. J., "Voids in Irradiated Stainless Steel," Nature, 216, Nov. 1967.

[3] Bloom, E. E., "An Investigation of Fast Neutron Irradiation Damage in an Austenitic Stainless Steel." ORNL-4580, August, 1970.

[4] Boltax, A. et al., "Fast Reactor Fuel Performance Model Development," Nuclear Applications and Technology, Vol. 9, Sept. 1970.

[5] Boltax, A. et al., "Mixed-Oxide Fuel Pin Performance Analysis Using the OLYMPUS Computer Code," Am. Nucl. Soc. Conference on Fast Reactor Fuel Element Technology, April 13, 1971, to be published.

[6] Mendelson, A., PLASTICITY: THEORY AND APPLICATION, The MacMillan Company, New York, 1968.

[7] Garafalo, F., FUNDAMENTALS OF CREEP AND CREEP RUPTURE IN METALS, MacMillan Co., New York, 1966.

[8] Mosedale, D., Lewthwaite, G. W., Leet, G. O., and Sloss, W., "Irradiation Creep in the Dounreay Fast Reactor," Nature, 224, 1301 (1969).

[9] Hesketh, R. V., "Collapse of Vacancy Cascades to Dislocation Loops," Proc. Intern. Conf. Solid State Physics Research with Accelerators, BNL-50083 (C-52) 389, Brookhaven National Laboratory (1967).

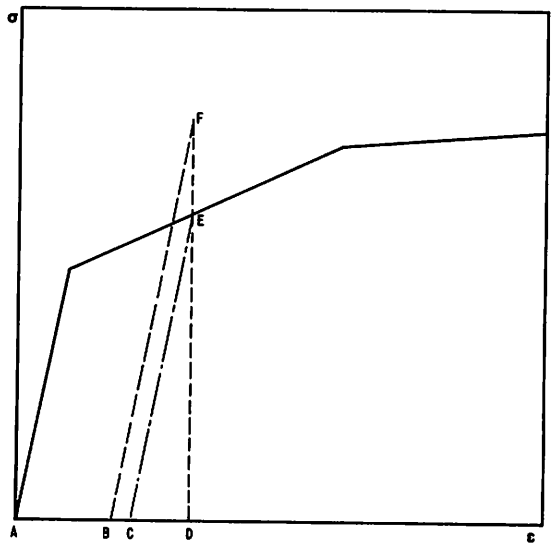

Figure 1. Plastic Strain Calculation

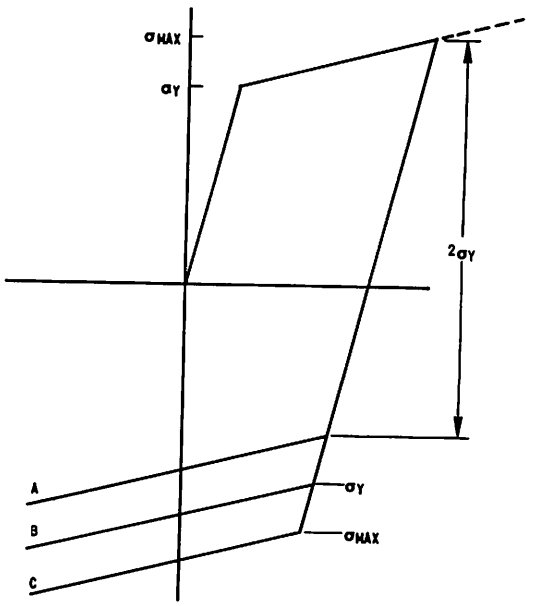

Figure 2. Reverse Loading Options

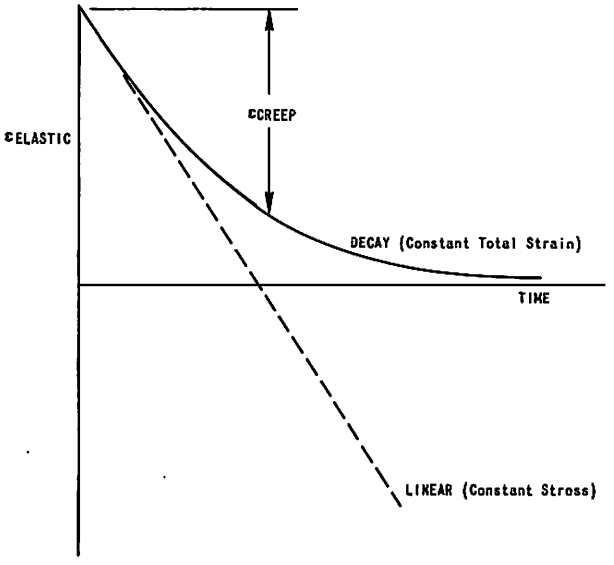

Figure 3. Creep Strain Options

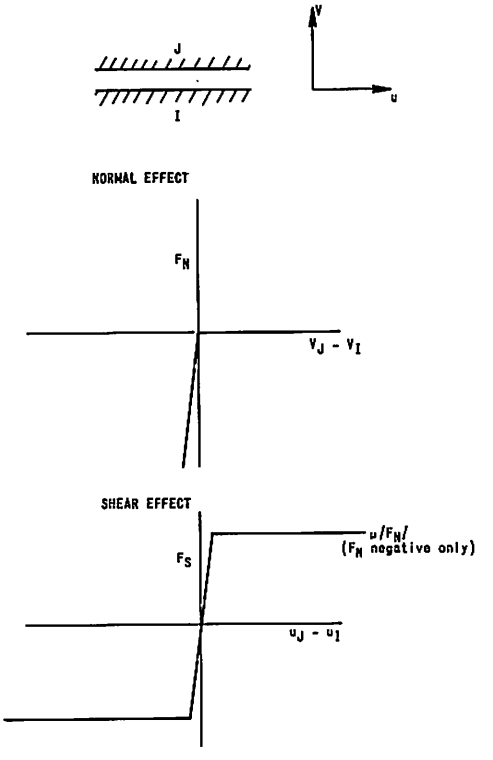

Figure 4. Interface Element Characteristics

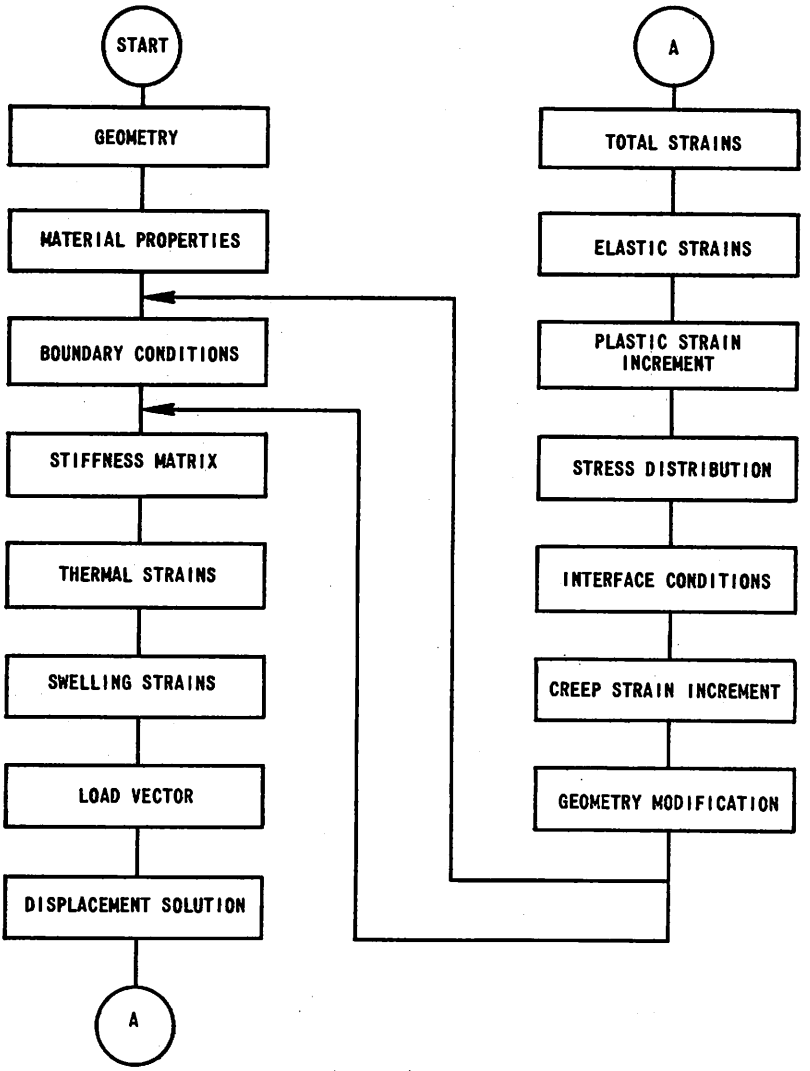

Figure 5. General Flow Chart for Non-Linear Analysis

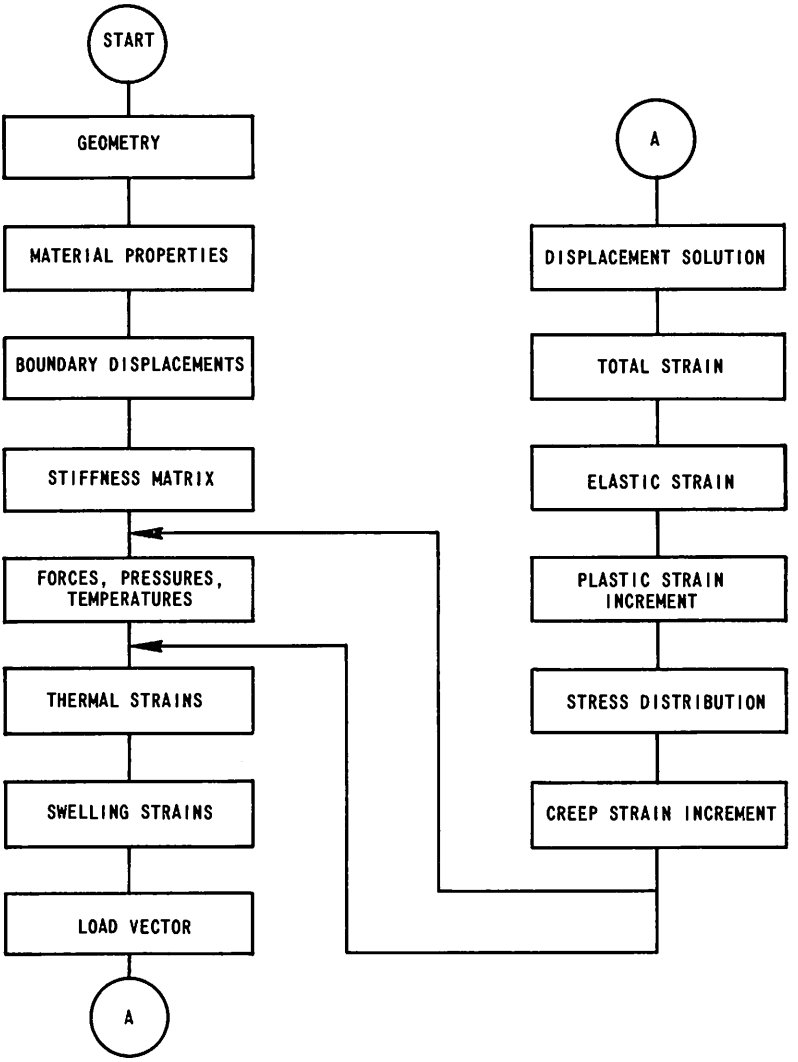

Figure 6. General Flow Chart for Simplified Non-Linear Analysis

4152-6

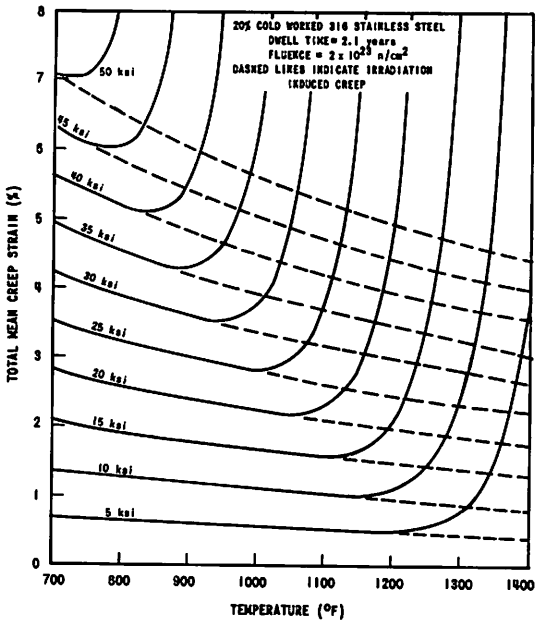

Figure 7. Thermal and Irradiation Induced Creep Strain Versus Temperature and Stress

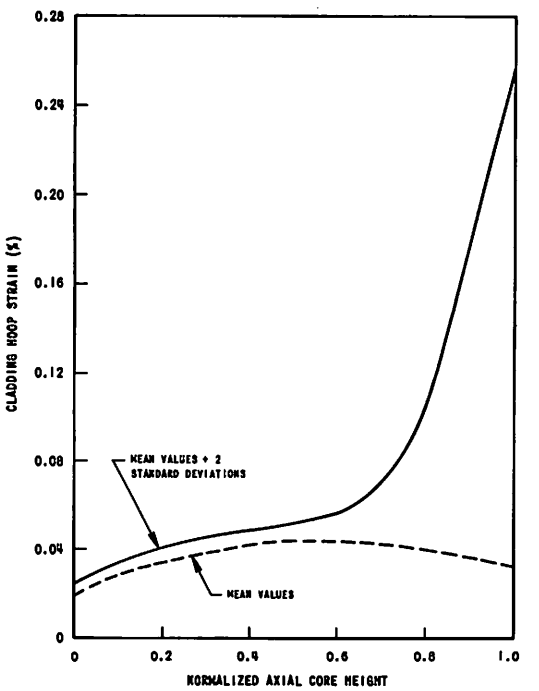

Figure 8. Axial Distribution of the Ductility Limited Cladding Hoop Strain

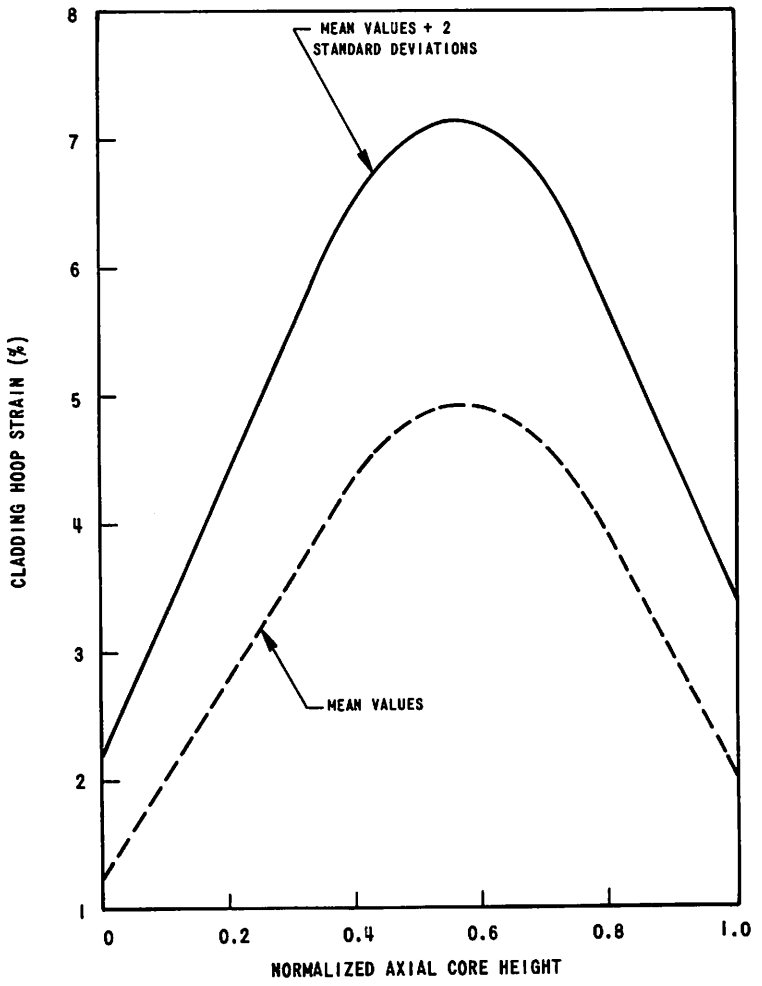

Figure 9. Axial Distribution of Total Cladding Hoop Strain

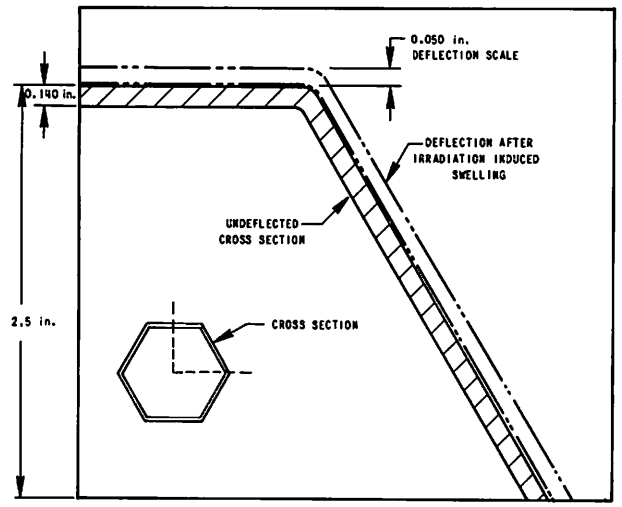

Figure 10. Duct Expansion Due to Irradiation Induced Swelling Only

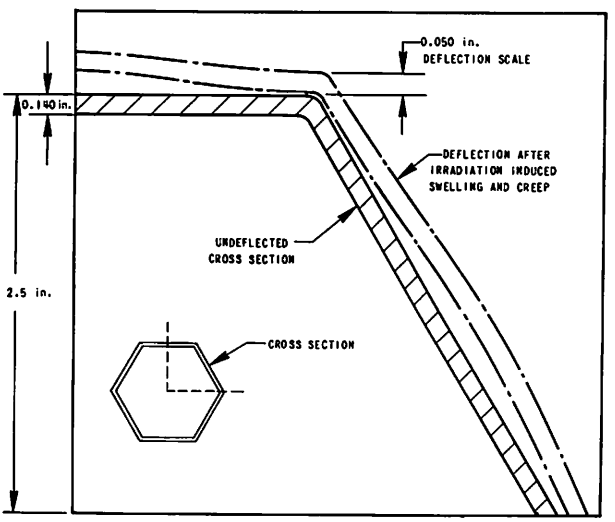

Figure 11. Duct Expansion Due to Irradiation Induced Swelling and Creep

DISCUSSION

Q K. WILLAM, Germany

Does your program provide the user with any information about the conditioning of your stiffness matrix (e. g. , in case interface elements are applied) for instance the conditioning number for estimating possible numerical errors during the solution process ?

A J. A. SWANSON, U. S. A.

The ANSYS program uses the wave front equation solver, in which the total stiffness matrix does not exist in its entirity at any time in the solution procedure, so no technique operating on the stiffness matrix has been included.
The user has simple guidelines for the selection of the interface stiffness such that the matrix is not ill-conditioned.
In a model set up by a qualified user conditioning of the stiffness matrix should be a problem only if the structure itself is poorly conditioned.
If a portion of the structure is in fact very rigid, the ANSYS capability for "coupled degrees of freedom" can be applied.

Q T. Y. CHANG, U. S. A.

The equation $\Delta\varepsilon=\varepsilon_{el}(1-e^{-\dot{\varepsilon}\Delta t})$ you have used in your creep analysis for estimating the time steps appears to be valid only for linear creep. What would be the case if the creep of material is a nonlinear function of stress ?

A J. A. SWANSON, U. S. A.

It is true that this equation is only strictly valid if the creep is a linear function of stress. For higher order functions in stress it is just another approximation, but still will be closer than the linear approximation for strain limited stress states.

Q E. KREMPL, U. S. A.

Equations (1), (3) in the paper are one-dimensional. How do you obtain a rule for three dimensions ? In what form are these rules used in the computer program ?

A J. A. SWANSON, U. S. A.

For three-dimensional analysis, generalized stress and strain are used in place of the one-dimensional stresses and strains given in these equations. The Von Mises yield criteria is used, along with Prandtl-Reuss equations.

Q W. L. GREENSTREET, U. S. A.

Does your method for doing plastic strain calculations require the use of an effective stress-effective strain diagram for combined stress states in all cases ?

A J. A. SWANSON, U. S. A.

Each stress state in the various types of plastic elements is combined to produce an equivalent stress-strain point. This stress-strain point is then compared with the input stress-strain-temperature characterization of the material to determine the increment of plastic effective strain occuring in the given load step. The appropriate form of the plastic flow rule is then used to calculate the components of the plastic strain increment to be added to each strain component.